UDK 669.714

V. Boyko[1], O. Prach[2], K. Mykhalenkov[2]

[1] The Technical university of Berlin, Berlin, Germany
[2] The National Technical University of Ukraine «KPI», Kiev, Ukraine

MELTING BEHAVIOR AND ARTIFICIAL AGING OF Al-Mg-Si-Mn NOVEL CASTING ALLOY CONTAINING Li

The strength of Al-Mg-Si-Mn-Li casting alloy strongly depends on Mg content in solid solution and precipitation of nano-size precipitates of β- Mg_2Si and δ- Al_3Li phases. Alloy with the nominal composition AlMg5Si2MnLi was studied by means of differential scanning calorimetry (DSC), transmission electron microscopy (TEM) and energy dispersive X-Ray analysis (EDX). DSC measurements show that the eutectic melting temperature was about 595 °C and it is higher than that of commercial A356 casting alloy. The macro- and microhardness tests show that in as-cast state hardness were higher than for A356 and continuously growth during artificial aging. TEM investigations reveal that during artificial aging three different precipitation types are forms in the alloy matrix. Two of them belong to the different structures of Mg_2Si precipitates. Appearance of the third one identified as δ- Al_3Li phase represent that Al-Mg-Si system can be successfully used for designing of Li-containing casting alloy which is not developed yet.

Key words: *cast Al-Mg-Si aluminium alloys, DSC, nanosize precipitation.*

1 Introduction

Automotive and aerospace industries are strongly interested in the development of new alloys for production of the light weight components and constructions. In this context Al-Mg-Si system are always considered as promising candidate for production of the sheets or extrusions owing to the combined merits of low weight and strong mechanical properties. This is true for wrought alloys where Al-Mg-Si alloys are the most popular ones and uses for body panels and frame parts. Only recently casting alloys of Al-Mg-Si system possessed increasing application in production of wide verity of car components, such as transmission housings, cylinder heads, inlet manifolds, engine sumps, brackets, heat sinks, stators, as well as for decorative trim items.

For production of the thin wall and high integrity casting the one of the most substantial competitor for well established Al-Si casting alloys, such as A356, is the recently recalled to life AlMg5Si2Mn alloy. To date it is established that Al-Mg-Si casting alloys possesses good corrosion resistance, weldability, high surface finishing and, in a particular case, extremely high mechanical properties in as-cast condition. It was reported by Koch et al. [1] that a Al-alloy with the nominal composition AlMg5Si2Mn subjected to high pressure die casting (HPDC) shows one of the best highest level of ductility (up to 18 %), yield strength (up to 220 MPa) and ultimate tensile strength (up to 350 MPa) compared with other casting alloys. It was established by Boyko et al. [2] that the origin of such a high properties of AlMg5Si2Mn in as-cast state is the formation of bI precipitates during natural aging. The mechanism responsible for the precipitates formation is the heterogeneous nucleation on dislocations.

From the beginning of the application of Al-Mg-Si casting alloys in foundry shops their ability to be strengthened by heat treatment is the matter of many controversies. The established data on the effect of solution treatment, quenching and aging is scanty and still attracts interest of researchers. Some authors stated that final properties of HPDC AlMg5Si2Mn alloy can be significantly increased by T6 heat treatment [3–6]. From the work of Petkow et al., [4] one can see that the AlMg5Si2Mn alloy, cast into permanent mold, shows only a slight increase of tensile and ultimate tensile strength after T6 treatment together with a dramatically low fracture elongation of about 2,5 %, and than decreasing down to 1,4% after artificial aging. The observed by Zhu et al. [5] relationship between properties in as-cast state, and following solution treatment for 8 hours at 570 °C and quenching, and an artificial aging at 190 °C for 8 hours resulted in an ultimate tensile strength of 263 MPa, which is even lower than that of A356 T6.

From the work of Jiang et al. [6] it can be deduced that the ultimate tensile strength of A356 T6 may reach a level up to 300 MPa and an elongation to fracture of 6 %. Comparable to A356 mechanical properties of permanent mold casting of AlMg5Si2Mn were reported in [7]. It was found that the ultimate tensile strength varies from 255 to 298 MPa and the elongation is in the range between 1,2 and 3,2 %. It has to be noticed that such a low elongation values is one order lower than that of AlMg5Si2Mn HPDC, where it can be as high as 18 %.

© V. Boyko, O. Prach, K. Mykhalenkov, 2013

It is known that Al-Mg-Si system belong to the group of age hardenable alloys and can be heat treated to achieve necessary conditions with appropriate strength, [4]. However, the optimal solution treatment temperature and time for artificial aging of casting alloys are not established yet.

Similarly to heat treatment, the effect for additional alloying of AlMg5Si2Mn, for example by Li, on the structure formation and mechanical properties is not yet considered too. From the early work of Fridlyander et al. [10] it is clear that addition of Li to Al-Cu or Al-Mg alloys can substantially enhance mechanical properties simultaneously with decreasing density. Last years showed strong advance in the development of the Al-Cu-Li and Al-Mg-Li wrought alloys. But, there is no one Li-containing casting alloy is designed up to now. It was proposed to use AlMg5Si2Mn casting alloy as the matrix to design Li-containing casting alloy with different Mg content and reveal the effect of Mg and Li on the alloys structure and precipitation of strengthening phases.

The main scientific approach to use Li addition is based on the composition of a-Al solid solution in AlMg5Si2Mn. During preliminary investigations it was measured that a-Al grains contains about 2,4 at.% Mg, 0,3-0,4 at.% Mn and no Si content detected. Subsequently, in a local scale α-Al grains of can be considered similarly to Al-Mg alloy where Li addition produces effective strengthening effect. Thus, the purpose of the present paper is to establish the melting behavior of Al-Mg-Si-Mn casting alloy with different Mg content and to find out the effect of Li on the its microstructure and hardness.

2 Materials and experimental procedure

The chemical compositions of alloys under consideration are represented in table 1. Commercial casting alloy A356 was used in present study for comparison.

All alloys subjected to research program were prepared in electric resistant furnace using graphite crucibles. As starting materials high purity aluminum (A99,997), AlMg50, AlSi25, AlMn26 and AlLi5 master alloys were used. Pure aluminum was charged into preheated up to 720 °C crucible. When Al become molten and overheated of 720 °C, preheated up to 350 °C AlSi25 and AlMn26 master alloys were added to the melt. After each addition the melt was stirred by titanium rod to avoid contamination of the melt by Fe. After additions of Mg and Li, the melt surface was covered by flux and then argon blowing lance was immersed into the melt. Argon blowing for 10 min was used to purify the alloy from nonmetallic inclusions and gases.

After flux treatment and argon blowing surface of the metal was skimmed to remove dross's with following pouring the melt into permanent steel mold. The mold temperature was 25 °C and kept constant for all castings. This casting condition gives cooling rate of 2 $K \times s^{-1}$ prior to solidification. The size of ingots was 160×25×17 mm. After complete cooling ingots were sectioned using high speed water cooled saw. Specimens for metallographic examinations with dimensions 10×10×10 mm were cut from the central parts of the ingots.

Two types of heat treatment were applied. The first one is the solution treatment, which was conducted in an electrical resistance furnace. Prior to heat treatment, a furnace was heated up to the necessary temperature and kept for 30 hours for establishing required thermal conditions. Temperature was controlled by a K-type thermocouple placed directly at the surface of the specimens. The melting temperature of each specimen was determined from differential scanning calorimetry runs. Soaking time from 20 min up to 24 hours was used for the solution treatment studies. The time for reaching the solution treatment temperature was 10–15 min and excluded from the total soaking time. After solution treatment the specimens were quenched in to the water with room temperature.

The second type of heat treatment was T6, which combines solution treatment at 570 °C (30 min, 1h and 1,5 hours), quenching in water with room temperature and artificial aging. Artificial aging was conducted in a forced circulation air furnace at 175 °C for various times. The time needed for heating the specimens up to the artificial aging temperature was 20 min and is excluded from the presented times. The specimens were taken out of the furnace and cooled in still air after artificial aging.

All TEM investigations were carried out using a TEM Philips CM 30, operated at 250 kV accelerating voltage and equipped with Energy Dispersive Spectrometry system (EDX) by Noran System Thermo Scientific. Thin foils were prepared using electrolytic thinning technique.

For investigation the specific temperatures of associated with melting of different phases differential scanning calorimeter NETZSCH DSC 404 was used. Heating rates was in the range 1–10 K min^{-1}. Li-contain specimens were heated under vacuumed to avoid oxidation. Specimens of commercial A356 alloy were heated in air.

Table 1 – Nominal composition of alloys in at. %(Al-balance)

alloy	Mg	Si	Mn	Li	Fe
L	5,52	1,91	0,29	3,79	–
B2	7,72	2,86	0,29	3,79	–
A356	0,36	6,71	0,01	–	0,03

Hardness measurements were performed using a Brinell hardness testing machine (HB) with a ball diameter of 2,5 mm and a load of 62,5 kg, time of loading was 10 sec. Microhardness tests were carried out on polished non-etched specimens on a Duramin-2 microhardness tester, HV 0,05 with standard indentation time.

3 Results and discussion

3.1 DSC analysis

Differential scanning calorimetry (DSC) is used in the present study to determine the melting and solidification characteristics, such as the onset temperatures of phase transformations. The specimen's masses were in the range from 0.01663 to 0.02134 g. Heating curves for L, B2 and A356 alloys are shown in Figure 1*a* and *b*.

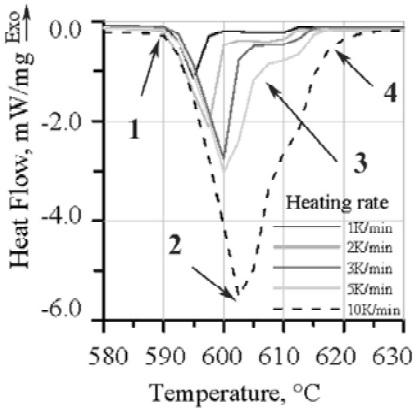

a

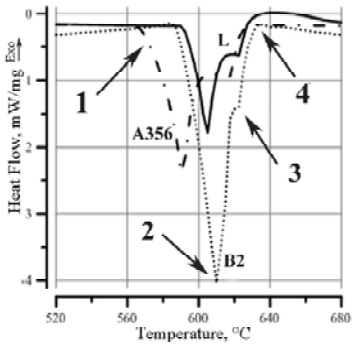

b

Fig. 1. Enlarged parts of the DSC heating curves for L obtained at different heating rates (*a*) and DSC traces for A356, B2 and L heated at a rate of 10K min^{-1} (*b*)

Figure , a illustrates the DSC heating curves recorded at different heating rates of 1, 2, 3, 5 and 10 K min^{-1} for the L alloy in comparison to heating curve of commercial A356 alloy. At a slow heating (1, 2, 3 and 5 K min^{-1}) the thermal effects are depressed and only when 10 K min^{-1} heating rate is used the four sharp endothermic reactions can be distinguished. The first thermal reaction during heating is clearly seen in the Fig.1b and denoted as 1. This is an endothermic effect with the peak onset of 571 °C observed on heating curve for A356 commercial alloy and it corresponds to the melting of (Al)+(Si) eutectic. This value is very close to that defined from equilibrium Al-Si binary phase diagram where eutectic undergo melting at 577 °C, [8].

For L and B alloys DSC tests shows first endothermic peaks at about 595 °C (denoted 2), which corresponds to the melting of (Al)+(Mg_2Si) eutectic. Experimentally measured value is absolutely coinciding with data of equilibrium ternary Al-Mg-Si phase diagram, [6]. Heat effect 2 detected in B2 alloy is much larger than that for L.

Further heating lead to the appearance of another endothermic peak which is attributed to the melting of б-Al (denoted 3). The temperatures of α- Al melting were found very close for A356, B and L alloys. End of melting, denoted 4, exhibit nearly the same T_{outset} temperatures about 630 °C for all alloys.

The results of DSC investigation are summarized in table 2. Comparing DSC results one can see that eutectic melting temperature found for L and B2 alloys are very close to one another but considerably higher than for A356 alloy. This means that the service temperature of Al-Mg-Si casting alloys can be several tens of degree higher than commercial casting alloys are used now. Addition of Li has no effect on the eutectic melting temperature.

3.2 Hardness measurements

From DSC results the temperature for solution treatment can be defined. For L and B alloys the highest solution treatment temperature was selected as 570 °C which is about 20 °C lower than eutectic melting temperature in Al-Mg-Si system. The artificial aging temperature for L, B2 and A356 alloys was selected on the same level of 175 °C.

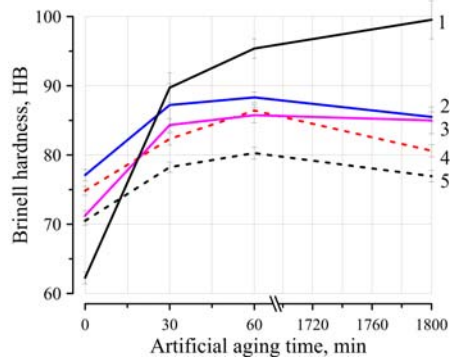

a

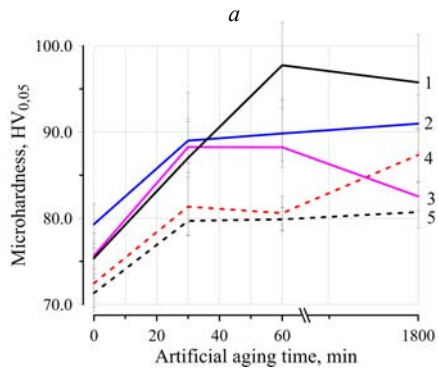

b

Fig. 2. Changes of Brinell hardness (*a*) and microhardness (*b*) of L, B2 and A356 alloys during artificial aging:
1 – A356; 2 – L solution treated for 90min, 3 – B2 solution treated for 90 min, 4 – L solution treated for 60 min, 5 – L solution treated for 30 min

Table 2 – Temperature characteristics of heat effects observed during heating

denoted	DSC	A356	L	B2
1	T_{onset}	571	594,3	595
2	T_{peak1}	590	605	610
3	T_{peak2}	617,5	620,8	620,3
4	T_{outset}	622,7	630	637,6

The results of hardness measurements are summarized in Figure 2 (*a*, *b*). One can expect that hardness of tested alloys should initially grow and than gradually decreases due to growth of β- precipitates and loss of their coherency with aluminum matrix. This is the most general tendency observed for all age hardenable aluminum alloys it is true for Al-Mg-Si or Al-Si-Mg alloys.

In as-cast state highest value of HB and HV0.05 was detected in B2 alloy. It was measured HB = 89 and $HV_{0,05}$ = = 97. Commercial A356 alloy showed slightly lover values of HB = 82 and $HV_{0,05}$ = 81. Solution treatment even for 30 min results in tangible decreasing of both HB and $HV_{0,05}$. After 30 min of solution treatment HB for B2 was detected of 70 and $HV_{0,05}$ = 75. Longer soaking lead to further hardness decreasing. Observed hardness decreasing is the result of two processes which simultaneously passes during heating. The first one is the eutectic spheroidization. The higher solution treatment temperature applied the quicker eutectic lamella broke into pieces and spheroidize. The second process is the dissolution of bI precipitates formed during natural aging. Details on the natural aging behaviour of AlMg5Si2Mn casting alloy can be found in [2].

After 30 min of artificial aging increasing of HB and $HV_{0,05}$ were detected for all alloys studied. Steep increasing of hardness was found for A356 alloy whereas for L and B2 specimens this change is not very sharp. After 90 min aging hardness reached maximum for L and B2 alloys and absolute values HB are in the range between 75 and 85, and $HV_{0,05}$ between 75 and 90. Prolonged aging up to 1800 min showed slight decreasing of HB for L and B2 alloys and gradual increasing for A356. Same hardness changes observed during $HV_{0,05}$ measurements.

3.3 TEM observation

Following the macro- and microhardness measurements, artificially aged specimens were the subject of TEM investigation. The main task was to analyze the composition of solid solution and detect precipitates formed via decomposition of super saturated solid solution. It is well established that in Al-Mg-Si alloys decomposition of supersaturated solid solution takes place during aging and precipitation sequence is SSSS→GP-I→β″→β′→ →β-Mg_2Si where SSSS is the super saturated solid solution and GP-I is the Guiner-Preston zones. This sequence is also true for A356 alloy where SSSS consists of Si and Mg.

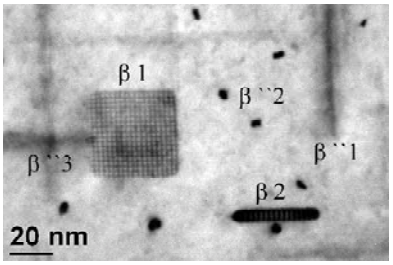

a

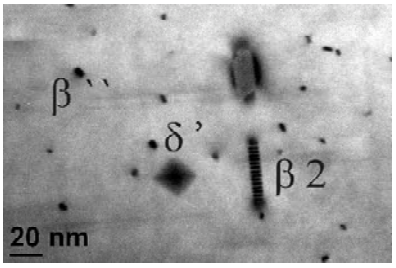

b

Fig. 3. Bright field image of β -Mg_2Si cuboid particles and β″ needles (*a*) and δ′- Al_3Li phase in L alloy after artificial aging at 175°C for 30 h

In figure 3 TEM bright field images of the L alloy artificially aged at 175 °C for 30 hours are shown. Three morphologies of precipitates can be clearly distinguished. The first one is the long needles lying in perpendicular directions and marked as $β''_1$ and $β''_3$. Fine black spots marked as $β''_2$ are the transverse section of needles. These precipitates are β″ phase which is the main strengthening phase of Al-Mg-Si alloys. Such needles were also observed in artificially aged A356 alloy and their appearance is obvious because the composition of solid solution is very similar to Al-Mg-Si alloys.

The second type of precipitates is the cubic shaped plates marked as β1. These precipitates are randomly

distributed in the matrix and have average dimensions of about 25×25 nm. Enlarged view of these precipitates is represented in figure 3a and shows two separate particles marked β1 and β2. Obviously, a quadratic, thin plate is positioned one time on its large face (β1), the other time it is in edge on position (β2). Thus the morphology of these precipitates is the thin plate and it can be identified as β-Mg_2Si cuboid particles. EDX analysis of cuboid particles showed that they enriched by Mg and Si simultaneously and this is an additional confirmation that these particles are Mg_2Si compound. It was reported by Ohmori et al. [9] that cuboid particles may form during decomposition of Si deficient solid solution. EDX measurements performed on L and B2 alloys showed that the average Mg content in solid solution in as-cast state is 2,7 at.%. Solution treatment for 90 min resulted in slight increasing of Mg content up to 3,1 at.% and later decreases down to 1,5 at.% after 30 min artificial aging. Simultaneously, Si content in solid solution in as-cast state and even after solution treatment was lower than the detection limit confirming that the solid solution in L and B2 specimens enriched with Mg and Si deficient which make formation of cuboid particles favorable. It was reported by Fridlyander et al. [10] that addition of Li decreases the solubility of Mg in α- Al. Since L and B2 alloys contain Li this can be additional factor fro promoting of formation of cuboid particles.

The third type of precipitates is the tetragonal shaped particles marked as δ′. Since both L and B2 alloys were alloyed with Li this precipitates can be identified as δ′- Al_3Li phase. These precipitates are formed along (111) aluminum direction and fully coherent with α- Al matrix. Appearance of δ′ precipitates and results of EDX analysis confirms the approach that the α- Al matrix in Al-Mg-Si alloys can be considered as binary Al-Mg alloy and addition of Li promote the formation not only Mg and Si containing precipitates but also δ′- Al_3Li phase. Details for all precipitation detected in Al-Mg-Si alloys containing Li are summarized in table 3.

Thus presence of Li in the solid solution affect on the formation of Mg-Si precipitates. Their heterogeneous behavior is linked to association of Mg-Si-v (vacancy) with Li-v clusters. The preferential clustering of Li-v inhibits the cluster of Si and Mg atoms, and retarding the diffusion of Si and Mg atoms so that the precipitation of needle shaped Mg_2Si phase is limited. Effect of the buffer for Li and Mg on the aging kinetics is slow increase of the Mg_2Si and the Al_3Li precipitates.

Conclusions

The results of the present study can be summarized as follows:

1. Temperature peaks of DSC study of the L and B2 samples have the same behavior, but the considerable difference in the value of heating flow. The eutectic melting temperature for two alloys was near 595 °C demonstrating that the Mg content has insignificant effect on the melting behavior of Al-Mg-Si alloys. Similar conclusion can be made for Li addition.

2. Both samples of AlMg5Si2Mn and AlMg7Si2Mn alloy showed the similar results of macro- and microhardness tests. The important point in this study is the 60 minutes of artificial aging, after this point all value extremely decrease, except for comparable A356 alloy in macrohardness investigation.

3. The addition of lithium has pronounced effect on the precipitation behavior in Al-Mg-Si-Mn alloys. The

Table 3 – Characteristics of precipitates in Al-Mg-Si and Al-Mg-Li systems

Al-Mg-Si	α_{SSS} →	GP zones →	β" →	β' →	β
composition		Si/Mg>1	Mg_9Si_5	Mg_9Si_5	Mg_2Si
unit cell			monoclinic a=0.650 nm b=0.760 nm c=0.405 nm γ=70°	hexagonal a=0.705 nm c=0.405 nm trigonal	cubic a=0.642 nm
shape	point defects	fine needle spherical 2nm	needle	rod/lath	cube
Al-Mg-Li	α_{SSS} →		δ' →	δ →	S_1
composition			Al_3Li	AlLi	Al_2MgLi
unit cell			cubic a=0.401	cubic a=0.638	cubic a=2.02
structure			$L1_2$	B32	–
shape	point defects		octagonal	cube	cube

TEM observation indicates three types of precipitations: β- Mg_2Si cuboid, β″- Mg_2Si needle shaped and δ′- Al_3Li tetragonal particle are forms during artificial aging

Finally, obtained results showed that using Al-Mg-Si alloy as the matrix the Li-containing casting alloy can be successfully designed and introduced into foundry practice as novel casting material with lower density.

Acknowledgement

The authors are grateful to thanks of the Visegrad Fund and the German Academic Exchange Service (DAAD) for supporting research included into this paper. Also, authors would like to thanks to Mr. Peter Grudde, KBM Affilips for supplying of lithium and magnesium containing master alloys.

References

1 H. Sternau «Magsimal-59 an AlMgMnSi-type squeeze-casting alloy designed for temper F» / H. Sternau, H. Koch, A. J. Franke //Aluminium Rheinfelden GmbH, P. O. Box 11 40, D-79601 Rheinfelden, Germany.

2 Microstructure characterization of AlMg5Si2Mn casting alloy / [Boyko V., Link T., Korzhova N., Mykhalenkov K.] // Materials Science and Technology (MS&T) 2013, October 27-31, Montreal, Quebec, Canada, 2013. – P. 1331–1338.

3. Wang Q. G. Solidification and precipitation behaviour of Al-Si-Mg casting alloys / Wang Q. G., Davidson C. J. // Journal of Materials science, 2001. – Vol. 36. – P. 739–750.

4. The precipitation sequence in Al-Mg-Si alloys / [Edwards G. A., Stiller K., Dunlop G. L., Couper M. J.] // Acta Meterialia, 1998. – Vol. 46, N 11. – P. 3893–3904.

5. Aging behavior of Li containing Al-Zn-Mg-Cu alloys / [Wei B. C., Chen C.Q., Huang Z., Zhang Y. G.] // Materials Science and Engineering, 2000/ – A280, P. 161–167.

4. Optimierung der Wдrmebenhandlung einer AlMgSi-Gusslegierung / [Petkov T., Kьnster D., Pabel T. etc.] // Druckguss, 2012. – Vol. 6, P. 268–274.

5. Effects of T6 heat treatment on the microstructure, tensile properties, and fracture behavior of the modified A356 alloys / [Zhu M., Jian Z., Yang G., Zhou Y.] // Materials and Design, 2012. – Vol. 36. P. 243–249.

6. Microstructure-based analysis of fatigue behaviour of Al-Si-Mg alloy / [Jiang X., He G., Liu B.] // Transactions of Nonferrous Metals Socity of China, 2011. – Vol. 2. – P. 443–448.

7. Wu L. Computer modeling of age hardening for cast aluminum alloys / Wu L., Ferguson G. // Materials Science and Engineering, 2009. – Vol. 4. – P. 2–6.

8. Mondolfo L.F. Aluminium Alloys: Structure and Properties. Butterworth & Co Publishers Ltd; 2nd Revised edition / Mondolfo L.F. – December 1979, 971 p.

9 Ohmori Y. Aging process in Al-Mg-Si alloys during contnious heating / Ohmori Y., Doan L.C., Nakai K. // Materials Transactions, 2002. – Vol. 43. – P. 246–255.

10. Влияние типа структуры на свойства холоднокатаных листов из алюминиевых сплавов / [Фриндляндер И. Н., Грушко О. Е., Берстенев В.В. и др.] // Технология легких сплавов, 2002. – № 4. – С. 4–14.

Одержано 06.02.2014

Бойко В., Прач Е., Михаленкова К. Особенности плавления и искусственного старения нового литейного сплава Al-Mg-Si-Mn, содержащего Li

Прочность литейных сплавов Al-Mg-Si-Mn-Li зависит от содержания Mg в твердом растворе и формирования наноразмерных выделений β- Mg_2Si и δ- Al_3Li фаз. Сплав с номинальным состав $AlMg_5Si_2MnLi$ был исследован с помощью дифференциальной сканирующей калориметрии (ДСК), просвечивающей электронной микроскопии (ПЭМ) и локального микрорентгеноспектрального анализа (ЛРСА). ДСК измерения показали, что температура плавления эвтектики в сплаве AlMg5Si2MnLi равна 595°C, что выше чем у коммерческого литейного сплава АК7. Измерения макро-и микротвердости показали, что твердость сплава в литом состоянии выше чему у АК7 и постепенно увеличивается в процессе искусственного старения. Исследования с помощью просвечивающего электронного микроскопа показали, что при старении три типа наноразмерных частиц формируются в матрице сплава. Два первых из них принадлежат к разным модификациям Mg_2Si фазы. Появление третьей фазы, идентифицированной как δ- Al_3Li, показывает возможность создания принципиально новых литейных Li-содержащих литейных сплавов, которые до сих пор не разработаны.

Ключевые слова: *Al-Mg-Si литейные сплавы, ДСК, нано размерные частицы.*

Бойко В., Прач О., Михаленкова К. Особливості плавлення і штучного старіння нового ливарного сплаву Al-Mg-Si-Mn, що містить Li

Міцність ливарних сплавів Al-Mg-Si-Mn-Li залежить від вмісту Mg у складі твердого розчину і формування наночастинок β- Mg_2Si і δ- Al_3Li. Сплав із номінальним складом $AlMg_5Si_2MnLi$ було досліджено за допомогою диференційної скануючої калориметрії (ДСК), трансмісійної електронної мікроскопії (ТЕМ) і локального рентгеноспектрального аналізу (ЛРСА). ДСК вимірювання показали, що температура плавлення евтектики в досліджуваному сплаві становить 595 °C, що вище за температуру плавлення евтектики в комерційному сплаві АК7. Вимірювання макро- і мікротвердості показали, що в литому стані досліджуваний сплав має більш високу твердість, ніж у АК7. До того ж, твердість поступово збільшується при штучному старінні. Дослідження за допомогою ТЕМ показали, що при старінні в матриці сплаву відбувається формування трьох типів частинок. Перші два типи належать до різних модифікацій Mg_2Si фази. Утворення третьої фази, яку було ідентифіковано як частинки δ- Al_3Li фази, засвідчує можливість створення на основі системи Al-Mg-Si принципово нових ливарних сплавів, які містять Li, і які ще не було створено до цього часу.

Ключові слова: *Al-Mg-Si сплави після лиття, ДСК, нано розмірні частинки.*